Power Beaming Project Beam Hopper Reflector Test Results

Anthony Baros and Brad Hoff (AFRL), Paul Pelletier (Leidos)

1. Introduction

The Air Force Research Laboratory, Directed Energy Directorate (AFRL/RD) is developing a novel wireless power beaming concept to provide new capabilities for electrical power transmission. In the concept under development, 95 GHz millimeter wave (MMW) electromagnetic radiation is transmitted over long distance wirelessly, through the air, as a focused beam. The MMW radiation is then captured by a heat exchanger system which converts the MMW energy to heat in order to drive a Stirling-type heat engine and 60 Hz low-frequency Alternating Current (AC) generator, by heating the Stirling engine working fluid. The heat exchanger utilizes novel susceptor ceramics which heat due to dielectric loss mechanisms when the MMW beam is applied. So, through this concept a transmitted MMW beam produces standard-frequency AC power at a distance up to 1 km.

To demonstrate the overall concept, an experiment is being devised utilizing a high-power MMW beam to drive the Stirling Engine/AC generator operation, via the heat exchanger, at a distance of 350 m. The source of the MMW beam is an Active Denial System (ADS), borrowed for use in this experiment. One issue is that a large (roughly 10x) disparity exists between the ADS beam size at the 350 m test distance and that of the heat exchanger susceptor ceramic absorbing surface area. Because we are interested in maximizing the amount of MMW directed onto the heat exchanger absorbing surface, a beam collector system, which we henceforth refer to as the beam hopper (since it somewhat resembles a grain hopper), was developed to concentrate the normal ADS beam to a smaller size, thereby increasing the MMW power density and total power applied to the heat exchanger. See **Figure 1** for a sketch of the overall concept, and **Figure 2** for the custom heat exchanger system developed for this effort.

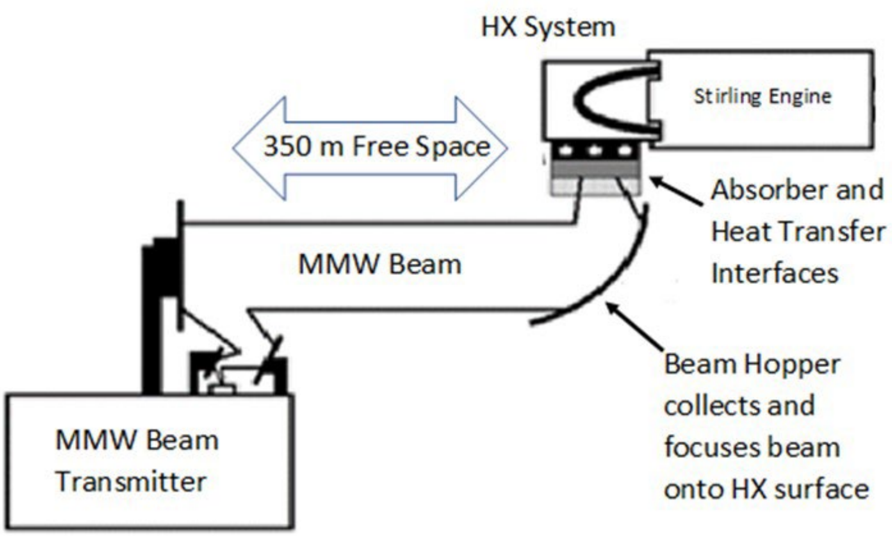

Figure 1: MMW Power Beaming Experimental Concept

Figure 2: Heat Exchanger (HX) system

2. Beam Hopper Design

The hopper reflector was designed to capture a large portion of the transmitted Radio Frequency (RF) beam and redirect/concentrate it onto the much smaller heat exchanger susceptor ceramic array. At the bottom of the beam hopper, the MMW-absorbing ceramic susceptor surface of the HX will be located to receive the concentrated beam. The beam hopper was fabricated mainly from sheet metal. The design's overall size was a compromise between percentage of ADS beam it would capture, and practicality in fabricating, transporting, and ruggedness for utilizing it during the outdoor experiment. The final design was also simple, low-cost, and comprised of easily-replaceable materials. Prior to fabrication, the design was simulated to verify expected performance. Simulation results and comparison with experimental performance will be discussed later. **Figure 3** shows the beam hopper before installation, and after being integrated together with the HX (not viewable in this photo) and the Stirling system. Note that in this test described herein, we did not attempt to heat the HX surface or run the Stirling engine; rather, we just wanted to measure the beam hopper performance.

Figure 3: Beam Hopper (left) and after integration with HX & Stirling System. The Beam Hopper dimensions are 1.9 m high by .84 m wide

3. Beam Hopper Performance Simulation

Simulations of the beam hopper performance were performed by the Leidos Electromagnetics group in St. Petersburg, FL. They used the High Frequency Structure Simulator (HFSS) ray tracing capabilities to model/simulate the beam hopper reflector system. ANSYS HFSS is a 3D Electromagnetic simulation software used for the design of RF systems and microwave devices. It includes tools for quick and very accurate electromagnetic simulations. It uses finite element method analysis, method of moments and ray tracing simulation methods depending on the requirement. HFSS uses Shoot and Bounce Ray tracing (SBR+) as geometric optic code along with the structures conducting surfaces to calculate the E, H and Poynting vector field intensities from reflected rays. **Figure 4** shows the hopper reflector structure model, ray tracing simulation, and calculated power density beam hopper output.

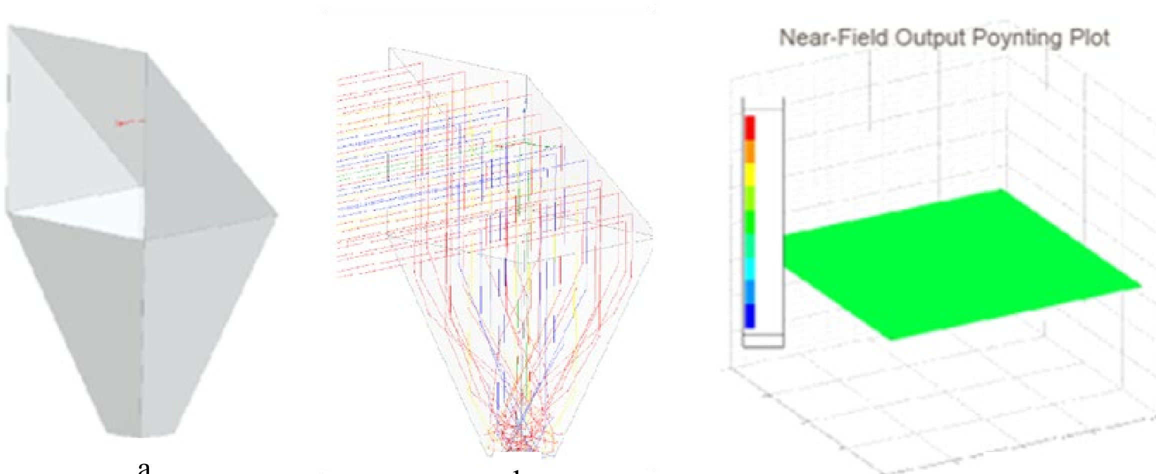

a b c

Figure 4: Beam hopper simulation geometry a), ray traces b), and target surface E-field map c).

In the simulation, the RF source was approximately 250 meters (experiment was 365 meters) away from the structure. Ray density during the simulations were $0.5{*}\lambda_{wave}$. Rays were reduced in number in **Figure 4** for demonstration purposes.

To reduce setup time, the modeler entered the RF beam as a 95 GHz, 100 kW plane wave and assumed it was in vacuum. This monochromatic wave propagates in the -$\hat{x}$ axis perpendicular to the opening. HFSS displays the electric field as it interacts with target surfaces. Reflected rays from the simulations are displayed in **Figure 4**. The number of bounces a ray takes to either reach the target or exit the horn is displayed as different colors; Green = 1, Blue =2, Yellow 3, Red > 4 bounces. To determine the power density, the modeler inserted a simulated near-field EM probe placed above an RF absorber material placed at the output/target. The simulations predicted an average power density of 55 W/cm^2.

4. Test Setup

Over the course of two test days, the Active Denial System 1R (ADS-1R, shown in **Figure 5**) was used to test the beam hopper system developed for the AFRL millimeter wave (MMW) power beaming effort. These initial check-out tests of the beam hopper had been planned for some time but were awaiting the repair of the ADS-1R source for completion. ADS-1R is similar to the ADS units described in [1].

Figure 5: ADS-1R High Power MMW Source

In both days of testing, the ADS-1R source was positioned 365 m away from the beam hopper. The beam hopper was attached to the Stirling engine system, with the bottom of the beam hopper intended to surround the HX surface. On the first test day, there was an imperfect fit, with a resultant gap—see item d., in next Section, and **Figure 6**. This was later corrected for the second day of testing. A thermal imaging sheet comprised of Carbon Loaded Teflon (CLT) was placed over the HX surface (located at the bottom of the beam hopper, where the concentrated power is directed). This material heats due to the MMW radiation directed onto it from the beam hopper. A thermal camera was used to measure the heating of this CLT sheet that occurred from a given shot, from which total power incident onto the CLT could be inferred. A complete explanation of this MMW power-measuring technique is available in [2]. With this setup, we directed MMW beam shots from ADS-1R into the opening of the beam hopper, through the hopper and onto the CLT target to test the beam hopper performance.

5. Test Limitations

In general, the limitations of this particular test that affected the results are anticipated to be reasonably minor towards the final results but are included here for completeness. Some of these were present during the first day of testing, then later addressed for the second day. The test limitations were as follows:

a. Non-optimal beam shape: At the time of these tests, ADS-1R suffered a problem causing a non-circular beam shape at the test location. Images are shown below in the Section 5: “Results” section. This test limitation was present for both test dates. The non-circular beam shape was anticipated to result in degraded performance of the beam hopper.

b. Targeting: ADS-1R operators were somewhat unfamiliar with ADS-1R provisions for improving beam targeting accuracy. This situation was somewhat improved upon during the second test date.

c. During the first day of testing, due to thermal camera positioning (at the top of the beam hopper, looking downward through the main opening at the CLT target at the bottom), a portion of the thermal image generated from the CLT thermal imaging target at the bottom of the beam hopper was clipped. This situation was resolved by redesigning the mounting bracket during the second day of testing, increasing the accuracy of the results.

d. Non-ideal fit of beam hopper to HX surface: A large gap (up to 2”) was found to exist between the bottom of the beam hopper and the surface of the HX absorber ceramic cylinders, where the CLT thermal imaging target to determine MMW power levels was placed. This allowed some MMW radiation to escape out into the surroundings, rather than being absorbed by the thermal imaging target. This gap was addressed for the second test day, to maximize the amount of MMW power onto the HX absorber ceramic cylinders (see **Figure 6**).

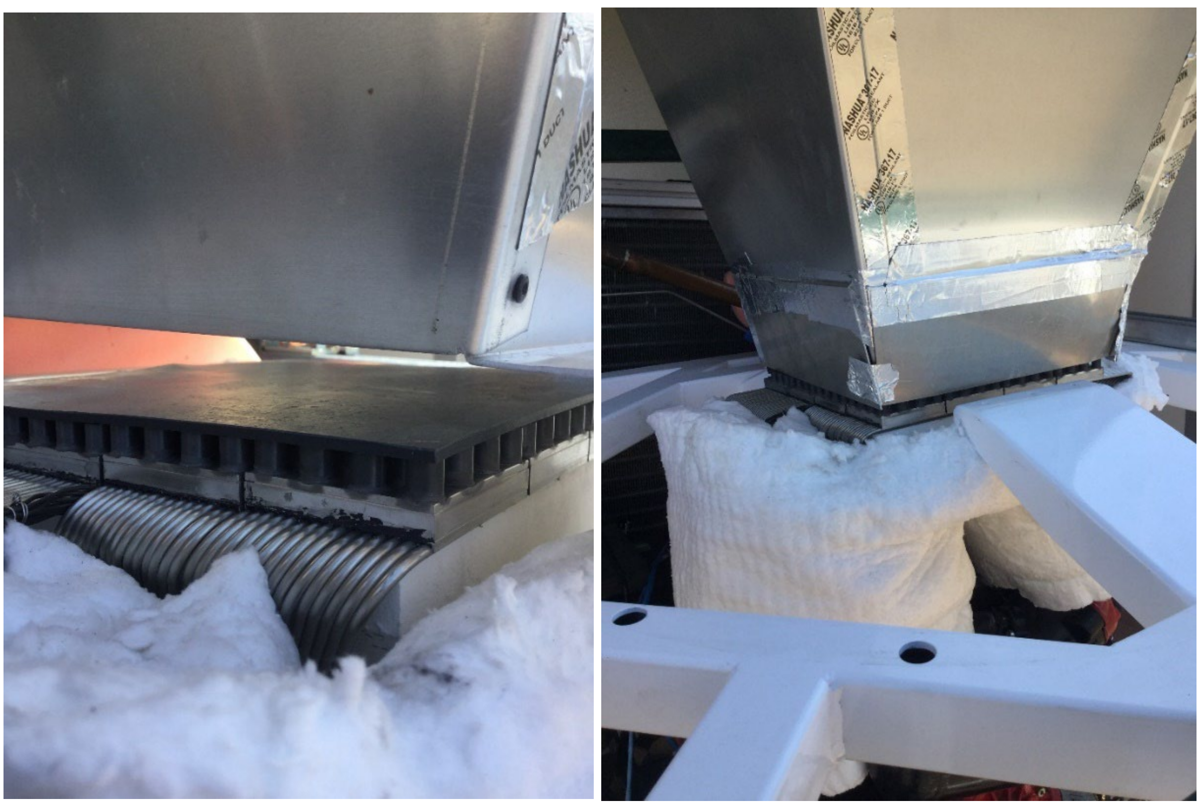

Figure 6: CLT imaging target placed on top of HX absorber cylinders. On Day 1 testing, note large gap between CLT/HX and bottom of beam hopper structure (left image). The gap was then corrected for the test on Day 2 (right image)

6. Results

a. Results—First Test Day (all test limitations present as described in Section 3)

All shots were two seconds in duration. At the time of this test, ADS-1R was producing an elongated beam (it should normally be circular), as well as a large side-lobe; these were due to some alignment faults at the time. See **Figure 7** for an image of the beam directed into the hopper.

For the "main beam lobe" directed into the beam hopper opening, beam parameters were measured as:

- Peak Power Density (Pd) = 8.1 W/cm^2
- Average Pd (33" x 33" square centered on the RF peak) = 4.5 W/cm^2
- Total Power in 33" x 33" square *(size of beam hopper opening)* centered on the RF peak = 31.3 kW

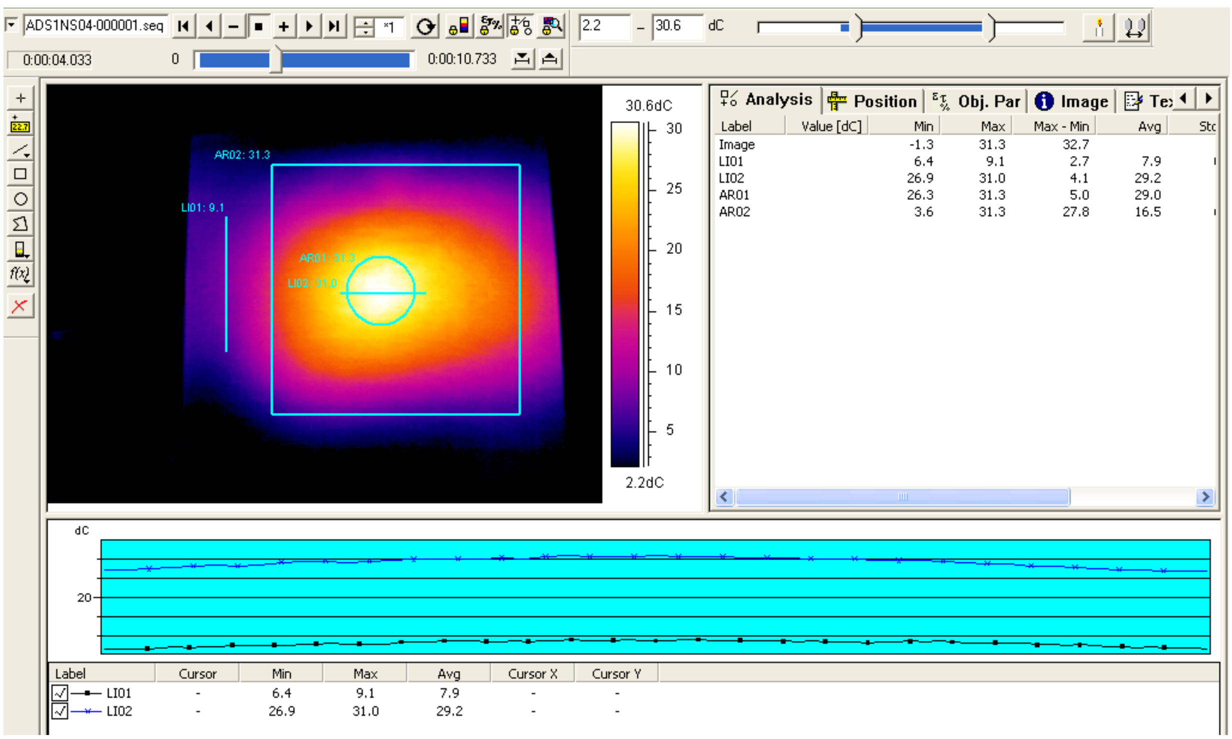

Figure 7: ADS-1R, 100%, 2 Second, RF Beam at 365 meters

We performed a calibration on a 10.25" x 9.25" section of CLT used to measure the beam hopper power. To do this, the hopper CLT was attached to a 4' x 4' calibrated CLT, centering the hopper CLT right edge on the center of the ADS-1R RF beam. See **Figure 8**.

From this, we determined the calibrated power density ratios (avoiding the edge thermal error effects). We determined the beam hopper CLT imaging target temperature increased by 1.2 times higher than the calibrated CLT's temperature rise. So, this calibration factor was used in calculating final numbers when determining beam hopper output power.

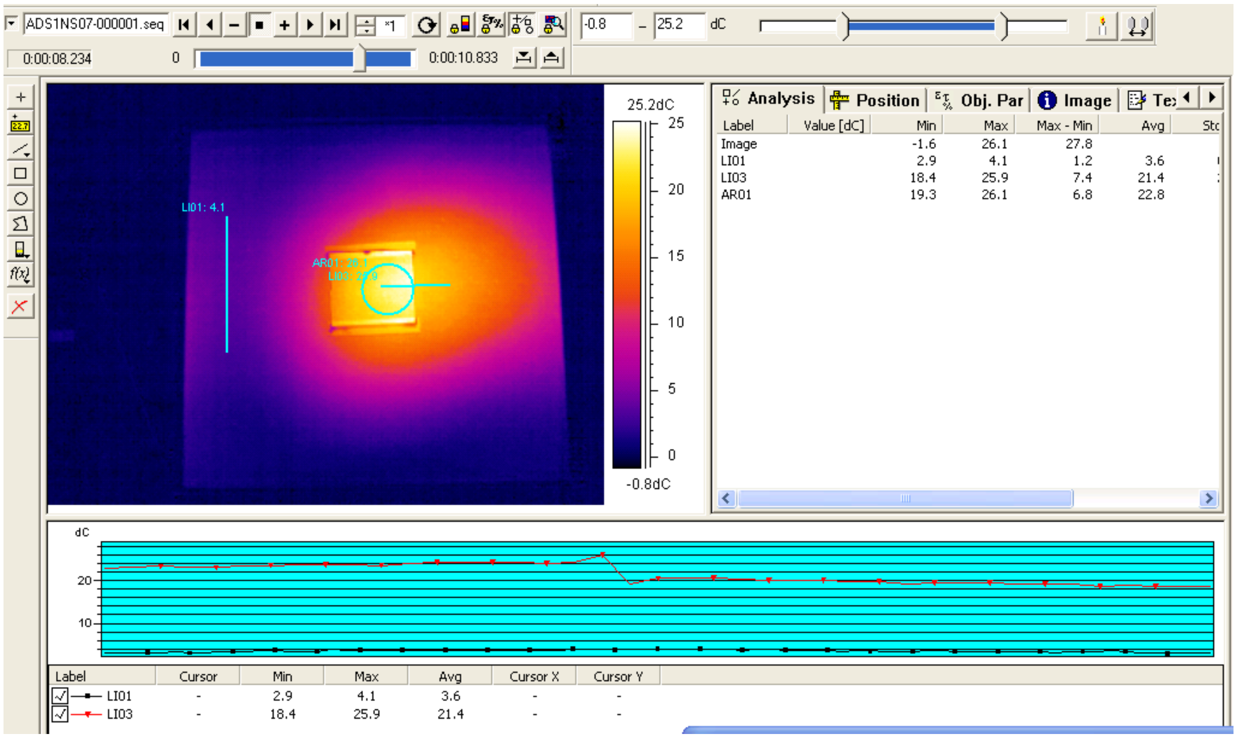

Figure 8: Hopper CLT Calibration

After calibration of the hopper CLT, we then placed it on top of the HX absorber ceramics under the beam hopper (as shown in **Figure 6**). There was a gap between the bottom of the beam hopper and the top surface of the hopper CLT of between 1.25” and 2”. We also noted that the surface of the ceramics were not perpendicular with the Stirling Engine support frame.

We then set up a Forward-Looking Infra-Red (FLIR) camera to look down into the beam hopper, to perform the thermal imaging of the hopper CLT. We again fired 100% (output power setting from ADS-1R), 2-second shots. We took thermal images of the CLT/inside walls of the beam hopper, an example of which is shown in **Figure 9**. The direct image of the CLT in Figure 8 is the portion with the blue box surrounding it. The rest of the images seen are IR reflections from the inside walls of the beam hopper. The CLT imaging was not complete; in our test, on this day, it was clipped due to the placement of the camera. This situation was corrected in the second day testing, to improve the accuracy of the estimated power on the hopper CLT. In the case of our described results here, for this day, our calculations assumed the thermal increase in the clipped, unmeasured section of CLT averages the same as the unclipped, measured CLT section.

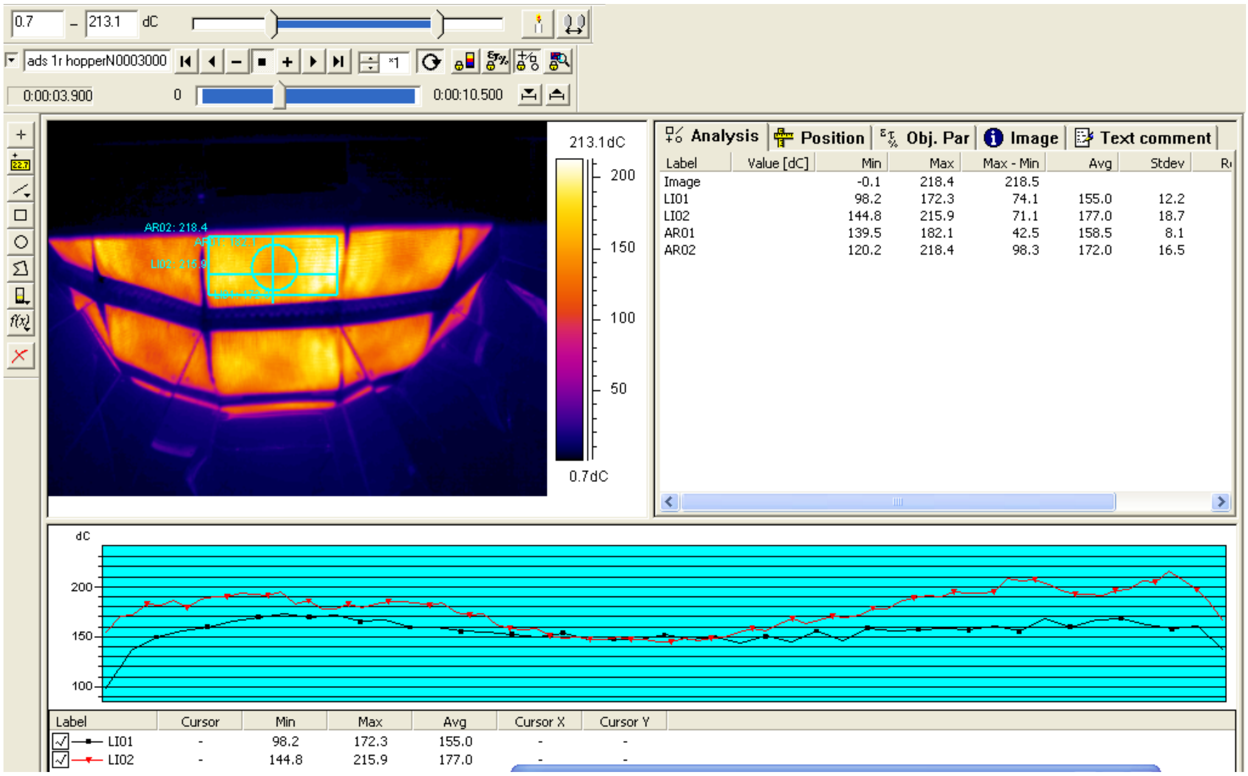

Figure 9: FLIR image of hopper CLT (with multiple mirror images due to interior beam hopper reflective surfaces)

The peak power density measured on the hopper CLT, including the correction factor found during the described calibration procedure, was 44 W/cm^2 with an average power density across the hopper CLT of 34.6 W/cm^2. From this, we calculated the estimated total power on the hopper CLT was 21.1 kW.

Results from testing on Day 1: An estimated 67% of the total power at the beam hopper opening was measured on the CLT target (placed directly on the top of the HX absorber ceramics). 31.3 kW measured in the 33"x 33" beam hopper opening area and 21.1 kW measured on hopper CLT target.

b. Results—Second Test Day (some test limitations remained as described in Section 3)

All shots were two seconds in duration. At the time of this test, ADS-1R was producing an elongated beam (it should normally be circular), as well as a large side-lobe; these were due to some alignment faults at the time. See **Figure 10** for an image of the beam directed into the hopper.

For the "main beam lobe" directed into the beam hopper opening:

- Peak Power Density (Pd)= 10.9 W/cm^2
- Average Pd (33" x 33" square centered on the RF peak) = 5.2 W/cm^2
- Total power in 33" x 33" square (*size of beam hopper opening)* centered on the RF peak = 36.5 kW

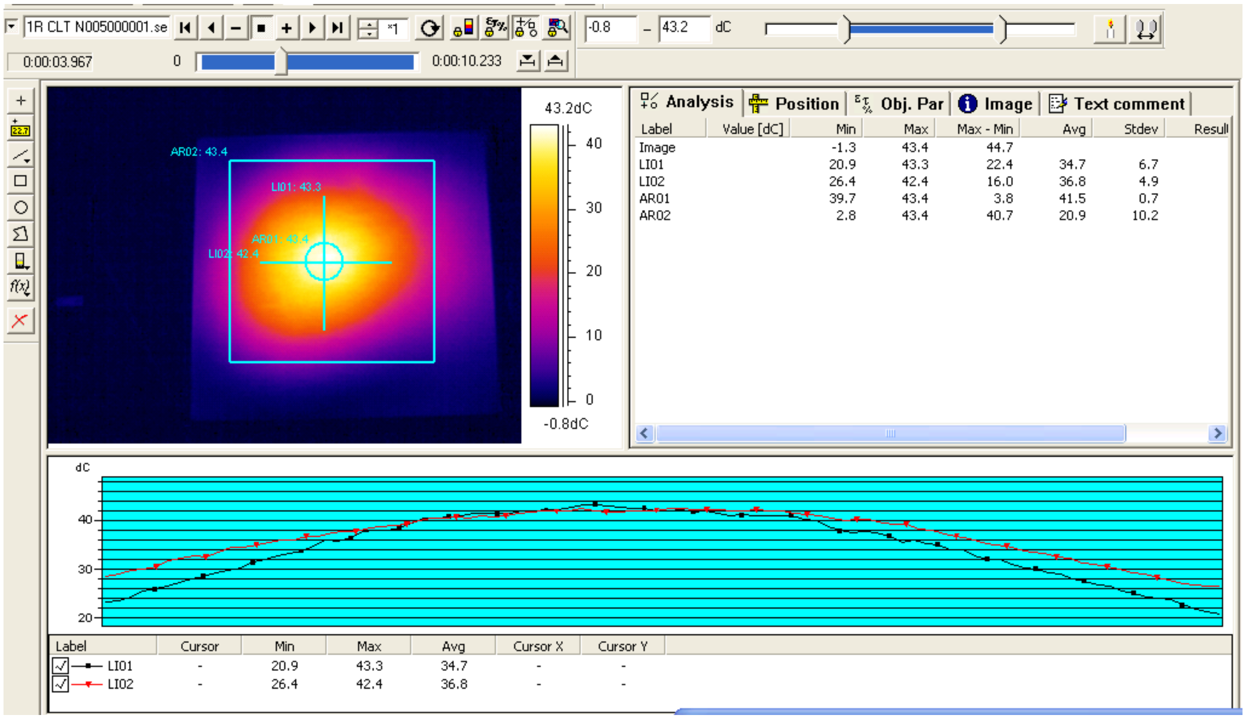

Figure 10: ADS-1R, 100%, 2 second, RF beam at 365 meters

We repeated the calibrations procedures on the hopper CLT, described in First Day testing. See **Figure 11**.

From this, we determined the calibrated power density ratios (avoiding the edge thermal error effects), which was 0.8 (hopper CLT power density to 4’ x 4’ calibrated CLT power density). The first-day testing showed the power density increase was linear with the temperature delta over short time periods.

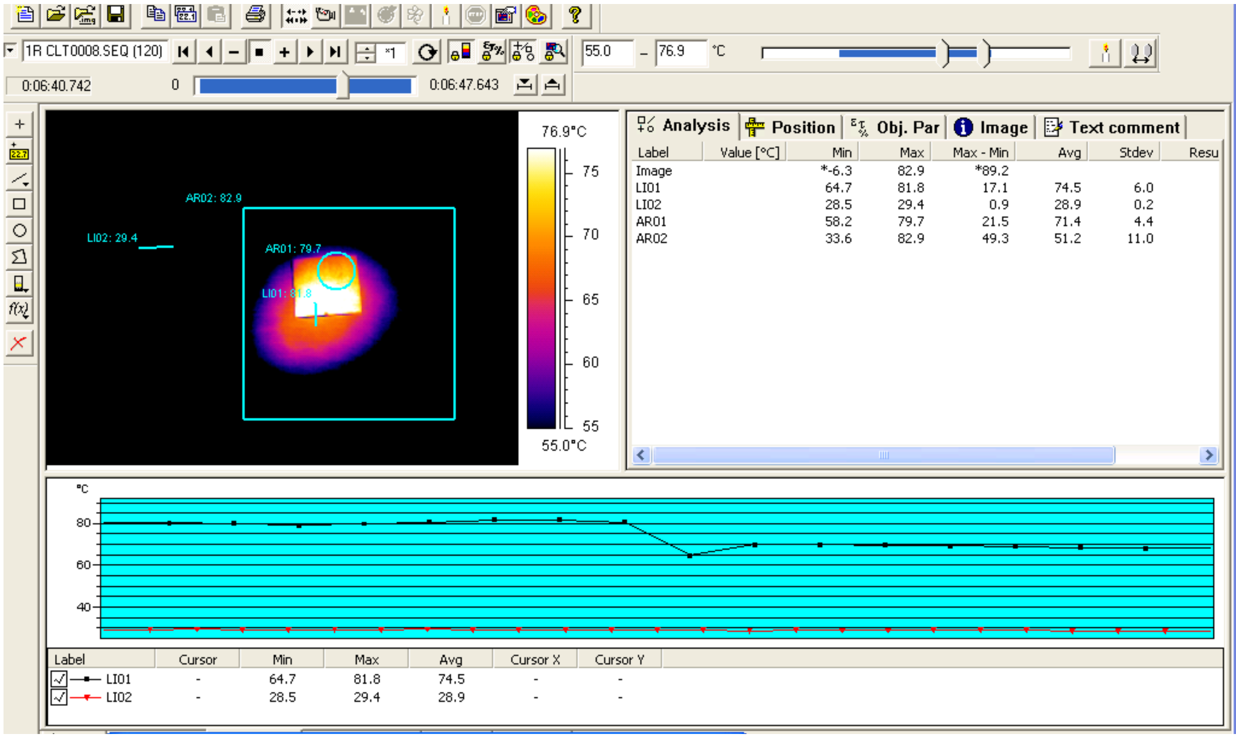

Label	Value [°C]	Min	Max	Max - Min	Avg	Stdev
Image		*-6.3	82.9	*89.2		
LI01		64.7	81.8	17.1	74.5	6.0
LI02		28.5	29.4	0.9	28.9	0.2
AR01		58.2	79.7	21.5	71.4	4.4
AR02		33.6	82.9	49.3	51.2	11.0

Label	Cursor	Min	Max	Avg	Cursor X	Cursor Y
LI01	-	64.7	81.8	74.5	-	-
LI02	-	28.5	29.4	28.9	-	-

Figure 11: Hopper CLT calibration

After calibration of the hopper CLT, we then placed it on top of the HX absorber ceramics under the beam hopper (as shown in Figure 2). On this second day of testing, the large gap between the bottom of the beam hopper and the top surface of the hopper CLT was largely addressed. To do so, we made adjustments to the hopper reflector height, perpendicularity, and camera placement, thus eliminating the large gap between the horn and target array, incident angle, and hopper CLT blind spot.

We then set up the FLIR camera to look down into the beam hopper, to perform the thermal image of the hopper CLT. We fired 100% (ADS-1R peak output power), one-second shots. We took thermal images of the CLT/inside walls of the beam hopper, an example of which is shown in **Figure 12**. The direct image of the CLT in Figure 11 is the portion with the blue box surrounding it; the rest of the images seen are reflections from the inside walls of the beam hopper. In this second day of testing, we corrected the camera imaging and captured the entire hopper CLT image, thus improving the accuracy of the test results, compared to the first-day test.

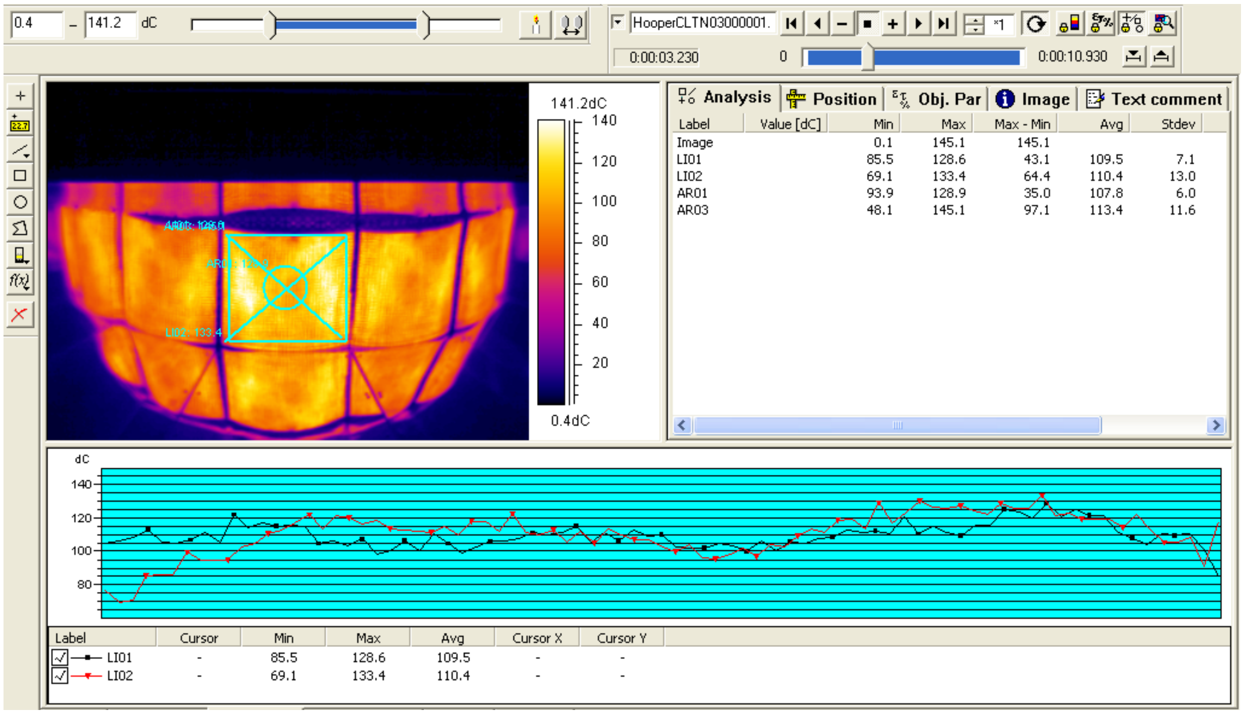

Figure 12: FLIR image of hopper CLT (with multiple mirror image on inside hopper reflector surfaces)

The peak power density measured on the hopper CLT, including the correction factor found during the described calibration procedure, was 42 W/cm^2 with an average power density across the hopper CLT of 37 W/cm^2. From this, we calculated the estimated total power on the hopper CLT was 23 kW.

Results from Day 2 testing: An estimated 63% of the total power at the beam hopper opening was measured on the hopper CLT target (placed directly on top of the HX absorber ceramics). 36.5 kW was estimated as entering the 33" x 33" beam hopper opening, and 23 kW was estimated on the hopper CLT target.

7. Conclusion and Future Plans

Conclusion: On our second day of testing, the results of which have higher accuracy, an estimated 63% of the total power at the beam hopper opening was measured on the CLT target (placed directly on the top of the HX absorber ceramics). Comparing simulation and experimental results, the simulation predicted much a higher average power density of 55 W/cm^2 at the hopper CLT, compared to what was seen experimentally, 37 W/cm^2. Better accuracy in the simulated vs actual results is obtainable by including accurate atmospheric loss factors and more-representative RF input beam parameters, including total MMW power in the beam, and the beam's shape. For example, just reducing the total power in the simulated transmitter beam from 100 kW to the actual estimated beam output power, to be more representative of the actual transmitted beam power, would have reduced the predicted average power density from 55 W/cm^2 to 47 W/cm^2. Still, accounting for the limitations in the model compared to the experimental setup, the agreement is overall reasonable.

Based on the experimental results seen, we anticipate the hopper performance will be sufficient to complete the AFRL power beaming test/demonstration and facilitate meeting the project's stated threshold goal of achieving 1 kW of AC power produced at a distance of 350 m away from the transmitting source.

8. References

[1] Levine, S., "The Active Denial System. A Revolutionary, Non-lethal Weapon for Today's Battlefield", *Defense Technical Information Center (DTIC)*, 2009

[2] J. Parker, C. Beason, & L. Johnson. "Millimeter Wave Dosimetry Using Carbon-Loaded Teflon". *Journal of Directed Energy*, Vol 6, No 4, pp 408-421., 2021